NASA TECHNICAL NOTE

NASA TN D-6544
C.1

NASA TN D-6544

BEHAVIOR OF Ti-5Al-2.5Sn ELI TITANIUM ALLOY SHEET PARENT AND WELD METAL IN THE PRESENCE OF CRACKS AT 20 K

by Timothy L. Sullivan

Lewis Research Center
Cleveland, Ohio 44135

NATIONAL AERONAUTICS AND SPACE ADMINISTRATION • WASHINGTON, D. C. • NOVEMBER 1971

1. Report No. NASA TN D-6544	2. Government Accession No.	3. Recipient
4. Title and Subtitle BEHAVIOR OF Ti-5Al-2.5Sn ELI TITANIUM ALLOY SHEET PARENT AND WELD METAL IN THE PRESENCE OF CRACKS AT 20 K		5. Report Date November 1971
		6. Performing Organization Code
7. Author(s) Timothy L. Sullivan		8. Performing Organization Report No. E-6345
9. Performing Organization Name and Address Lewis Research Center National Aeronautics and Space Administration Cleveland, Ohio 44135		10. Work Unit No. 124-08
		11. Contract or Grant No.
12. Sponsoring Agency Name and Address National Aeronautics and Space Administration Washington, D.C. 20546		13. Type of Report and Period Covered Technical Note
		14. Sponsoring Agency Code
15. Supplementary Notes		

16. Abstract

Through- and surface-cracked specimens of two thicknesses were tested in uniaxial tension. Surface-cracked specimens were generally found to be stronger than through-cracked specimens with the same crack length. Apparent surface-crack fracture toughness calculated using the Anderson modified Irwin equation remained relatively constant for cracks as deep as 90 percent of the sheet thickness. Subcritical growth of surface cracks was investigated. Comparison of chamber and "open air" welds showed chamber welds to be slightly tougher. Both methods produced welds with toughness that compared favorably with that of the parent metal. Weld efficiencies were above 94 percent.

17. Key Words (Suggested by Author(s)) Fracture mechanics; Cryogenic temperatures; Titanium alloy sheet; Titanium welds; Surface cracks		18. Distribution Statement Unclassified - unlimited	
19. Security Classif. (of this report) Unclassified	20. Security Classif. (of this page) Unclassified	21. No. of Pages 32	22. Price* $3.00

* For sale by the National Technical Information Service, Springfield, Virginia 22151

BEHAVIOR OF Ti-5Al-2.5Sn ELI TITANIUM ALLOY SHEET PARENT AND WELD METAL IN THE PRESENCE OF CRACKS AT 20 K

by Timothy L. Sullivan

Lewis Research Center

SUMMARY

An investigation was conducted to determine the behavior in uniaxial tension of the titanium alloy, Ti-5Al-2.5Sn extra-low interstitial (ELI) grade at 20 K (-423° F) when through and surface cracks are present. Tests were conducted to determine the effect on apparent surface crack fracture toughness K_Q of varying sheet thickness, specimen width, and surface crack dimensions. The sheet thicknesses tested were 1.5 and 2.8 millimeters (0.06 and 0.11 in.). The strengths of surface cracked specimens were compared with those of specimens with through cracks of the same length. Alloy toughness was determined in and near both chamber and inert-gas shielded "open air" welds. The extent of subcritical growth in surface cracks during loading to failure was investigated. Smooth properties of parent and weld metal at 20, 77, and 295 K (-423°, -320°, and 70° F) were also determined.

Although a few surface-cracked specimens failed at lower stresses than through-cracked specimens with cracks of the same length, this was not the usual behavior. In general, the surface-cracked specimens tested were stronger than ones with through cracks of the same length. Values of K_Q calculated by the Irwin method remained relatively constant for surface-crack depths up to 70 percent of the sheet thickness. Using a modification of the Irwin method by Anderson resulted in constant K_Q values for crack depths up to 90 percent of the sheet thickness. A significant amount of subcritical depth growth took place in the specimens as they were loaded to failure.

Good toughness levels were obtained in the weld metal. Chamber welded specimens were slightly tougher than those welded in open air. An unexplained loss of toughness was found in the heat affected zone of the thicker material tested. Good weld efficiencies were obtained by both weld techniques.

INTRODUCTION

The application of linear elastic fracture mechanics is presently quite limited when analyzing the effect of surface cracks in thin, relatively tough sheet material. This is especially true when trying to determine the effect of deep surface cracks on the strength of a structure. Irwin (ref. 1) developed an equation for calculating plane strain stress intensity K_I from surface-crack tests. However, Irwin recommended that its use be limited to surface cracks no deeper than half the sheet thickness. The usefulness of the Irwin equation is further limited by the requirements for valid K_{Ic} testing recommended by Brown and Srawley (ref. 2). In order to examine the usefulness of fracture mechanics concepts in an area of great interest to the designer, but outside the realm of valid K_{Ic} testing, an experimental investigation was conducted with a single alloy.

The alloy chosen for the experimental program was the titanium alloy, Ti-5Al-2.5Sn extra-low-interstitial (ELI) grade. This alloy is of interest as a cryogenic tank material for aerospace applications. Plane stress fracture toughness and other properties of this alloy were investigated by the author in several previous studies (refs. 3 to 6). Robelotto, Lambase, and Toy (ref. 7) investigated the effect of residual stress on the toughness of this alloy in and near welds at room temperature and at 200 K. Pyle, Schillinger, and Carman (ref. 8) tested heavier sections of this alloy to determine toughness in parent metal and in and near welds at 20, 77, and 295 K. In the present study the effects on apparent fracture toughness at 20 K of varying sheet thickness, test specimen width, crack length, and crack depth were investigated. The strengths of surface cracked specimens are compared with the strengths of specimens with through cracks of the same length. Because flaws are more likely to occur in welds, the toughness in and near welds of this alloy was also investigated. Both chamber and "open air" gas tungsten arc (GTA) welds were tested. Subcritical growth of surface cracks was investigated and its effect on the proof test logic discussed. Apparent fracture toughness values K_Q were calculated from the surface cracked specimen fracture data using both the Irwin equation and a modification of this equation developed by Anderson, Holms, and Orange (ref. 9).

Measurements and results are reported in the International System of Units (SI). Where necessary for clarity, U.S. Customary Units are also given. U.S. Customary Units were used for measurements and calculations reported herein.

TOUGHNESS CALCULATION METHODS

Surface-Crack Toughness

The stress intensity factor for a semielliptical surface crack in a plate subject to uniform tension was first developed by G. R. Irwin (ref. 1). The Irwin expression contains corrections for the effect of free surfaces and for the effect of small-scale yielding at the crack tip. The equation for the critical stress intensity factor or surface-crack fracture toughness K_{Ic} is given as

$$K_{Ic} = \sigma_c \sqrt{1.2\pi a/Q} \tag{1}$$

where Q is a crack shape parameter, equal to $\left[\varphi^2 - 0.212(\sigma_c/\sigma_{ys})^2\right]$ and

$$\varphi = \int_0^{\pi/2} \sqrt{1 - \left(\frac{c^2 - a^2}{c^2}\right)\sin^2\theta\, d\theta}$$

The other terms are defined as follows: a is the crack depth; c, the half crack length; σ_c, the gross stress at fracture; and σ_{ys}, the 0.2 percent offset yield stress. In equation (1), 1.2 is the free-surface correction factor; in the equation for Q, the term $0.212\ (\sigma_c/\sigma_{ys})^2$ corrects for the effect of plasticity at the crack tip.

Equation (1) is generally considered to be accurate for crack depths up to half the plate thickness and when yielding is confined to a small zone at the crack tip. Several attempts have been made to expand the range of usefulness of the Irwin expression. These equations take the general form

$$K_{Ic} = M\sigma_c \sqrt{\frac{\pi a}{\varphi^2}} \tag{2}$$

where M is a magnification factor to account for free surface and plasticity effects. Kobayaski and Moss (ref. 10) developed a magnification factor so that cracks deeper than half thickness could be used to calculate crack tip stress intensity. More recently, Anderson, Holms, and Orange (ref. 9) developed an expression for a magnification factor that is applicable until the plastic zone extends completely through the thickness. Because of their complexity, the magnification factors of references 9 and 10 are not repeated here.

Brown and Srawley (ref. 2) have proposed that certain minimum size requirements are necessary in order to calculate valid values of K_{Ic}. These minimum specimen and crack dimensions are multiples of $(K_{Ic}/\sigma_{ys})^2$ because the plastic zone size is proportional to $(K_{Ic}/\sigma_{ys})^2$. For surface cracks in thin, relatively tough sections, it is impossible to meet the proposed size requirements. Therefore, the values of fracture toughness calculated with equations (1) or (2) and reported herein cannot be considered valid values of K_{Ic}. They are apparent K_{Ic} and are identified herein as K_Q.

Through-Crack Toughness

The stress intensity factor for a through crack in a sheet subjected to uniform tension is again attributable to Irwin (ref. 11) and is given by

$$K_c = \sigma_c \sqrt{W \tan \frac{\bar{c}_c}{W}} \tag{3}$$

where

$$\bar{c}_c = c_c + \frac{1}{2\pi}\left(\frac{K_c}{\sigma_{ys}}\right)^2$$

and where c_c is the critical half crack length and W is the sheet width. If the more accurate secant width correction is substituted for the tangent correction of Irwin, the critical stress intensity factor or through-crack fracture toughness K_c is given by

$$K_c = \sigma_c \sqrt{\pi \bar{c}_c \sec \frac{\pi \bar{c}_c}{W}} \tag{4}$$

If subcritical crack growth is ignored, a nominal through-crack fracture toughness K_{cn} can be calculated by

$$K_{cn} = \sigma_c \sqrt{\pi \bar{c} \sec \frac{\pi \bar{c}}{W}} \tag{5}$$

where

$$\bar{c} = c + \frac{1}{2\pi}\left(\frac{K_{cn}}{\sigma_{ys}}\right)^2$$

and c is the original half crack length.

EXPERIMENTAL APPARATUS AND PROCEDURE

All the material for the tests conducted in this program came from a single heat of Ti-5Al-2.5Sn ELI titanium alloy. The material was rolled to two thicknesses: 1.5 and 2.8 millimeters (0.06 and 0.11 in.). After rolling, the sheet was annealed by heating to 1100 K (1500° F) for 5 minutes. The mill analysis provided by the supplier is given in the following table:

Sheet thickness, mm	Composition							
	Al	Sn	Fe	Mn	C	N	O	H
	wt. %							ppm
1.5	5.3	2.5	0.18	<0.01	0.02	0.007	0.098	40
2.8	5.3	2.5	.18	<.01	.02	.007	.091	34

Specimen Preparation

The various specimen configurations used in the test program are shown in figure 1. They apply to both parent metal and weld metal specimens. Welds ran transverse to the specimen loading direction and were machined flush with the adjacent material. Each specimen was made with its longitudinal axis parallel to the rolling direction of the sheet.

The type of test conducted with each configuration was as follows: specimens with 12.7-millimeter wide test sections (fig. 1(a)) were used to determine smooth properties.

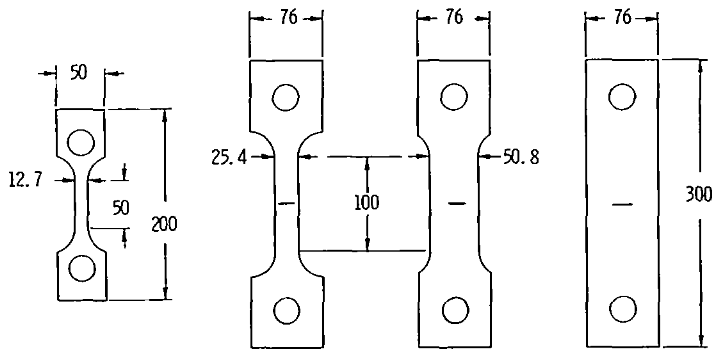

(a) 12.7 mm. (b) 25.4 mm. (c) 50.8 mm. (d) 76 mm.

Figure 1. - Test specimens (dimensions are in mm).

Specimens with 25.4- and 50.8-millimeter-wide test sections (figs. 1(b) and (c)) were used for surface-cracked and short through-cracked tests. Specimens with 76.2-millimeter-wide test sections (fig. 1(d)) were used for long through-cracked tests.

A crack was made by first placing a surface or through-thickness electrical discharge machined slot in the center of the specimen test section. Following slotting, the specimen was cycled at low stress until a crack of the desired length was obtained. The maximum cyclic stress was never greater than 40 percent of room temperature yield stress. Through cracks and most of the surface cracks were made by tension-tension cycling. This resulted in surface cracks with a crack depth to crack length ratio $a/2c$ of approximately 0.3. A few of the 1.5-millimeter thick parent-metal surface slotted specimens were cycled in bending. This produced surface cracks with values of $a/2c$ as small as 0.06.

Welding Procedure

Two GTA welding methods were used in preparing the weld specimens in order to compare a laboratory weld with a production weld. The first method used an inert-gas-filled chamber for protection. These welds were made at the Lewis Research Center. The second method used an inert-gas-shielded open air arc to simulate welding procedures more likely to be used in aerospace practice. The open air welds were made by an aerospace manufacturer. After the weld specimens had been machined, they were clamped flat and stress relieved by heating in vacuum to 870 K (1100° F) for 2 hours and furnace cooled.

Chamber welds. - The sheet for welding was prepared by shearing strips that were 152 millimeters (6 in.) wide by 456 millimeters (18 in.) long. The edges to be welded together were machined straight to provide a square butt joint. Just before welding, the edges were cleaned in an acid pickle, rinsed in water, and dried in air. The strips were clamped in a weld fixture and placed in the weld chamber. The chamber was pumped down and backfilled with argon gas.

The pieces were welded by a single pass on each side. A thoriated tungsten electrode was used and no filler material was added. A direct-current straight polarity power supply was used. With the 1.5-millimeter sheet the weld parameters were established to provide close to 100 percent penetration on each pass. These parameters were amperage, 55 to 60; voltage, 18 to 20; and weld speed, 152 millimeters per minute (6 in./min). With the 2.8-millimeter sheet, the weld parameters were established to provide slightly more than 50-percent penetration on each pass. This was obtained using an amperage of 110. The other parameters remained the same. Radiographic inspection of the welds showed a negligible amount of porosity.

Open air welds. - The sheet used for the open air welds was prepared in the same manner as that used for the chamber welds. Again a single pass was made on each side, a thoriated tungsten electrode was used, and no filler material was added. The weld was protected with a torch shield and trailing shield which supplied helium gas and a backing shield of argon gas.

Weld parameters for both sheet thicknesses were established to provide close to 100-percent penetration on each pass. For the 1.5-millimeter sheet these parameters were amperage, 75; voltage, 14; and weld speed, 76 millimeters per minute (3 in./min). For the 2.8-millimeter sheet the amperage was increased to 95 while the other parameters remained the same. Radiographic inspection of these welds showed slightly more porosity than was observed in the chamber welds.

Specimen Instrumentation and Testing

Specimens designed to determine the smooth properties of the parent metal were instrumented with an extensometer to provide 0.2 percent offset yield strength data. The same information was obtained from weld specimens by placing a strain gage on the weld metal portion of the specimen.

NASA continuity gages (ref. 12) were placed on the 76.2 millimeter-wide through-cracked specimens to measure subcritical crack growth. No attempt was made to measure subcritical crack growth on the 25.4- and 50.8-millimeter-wide through-cracked specimens.

No instrumentation was used on most of the surface-cracked specimens. However, to obtain some information about subcritical crack growth behavior of a surface crack, a few specimens were instrumented as follows: To detect length growth at the surface, continuity gages were placed at the crack tips. The use of these gages was discontinued after initial tests showed no surface length growth. To detect and gain a qualitative indication of depth growth, strain gages were placed over the crack and on the surface behind the crack. Because of the high local strain over the crack, it was necessary to develope a gage mount like that shown in figure 2 to prevent failure of the gage before

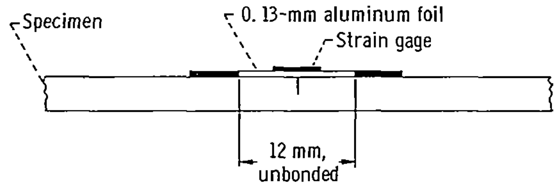

Figure 2. - Over-crack strain gage mount.

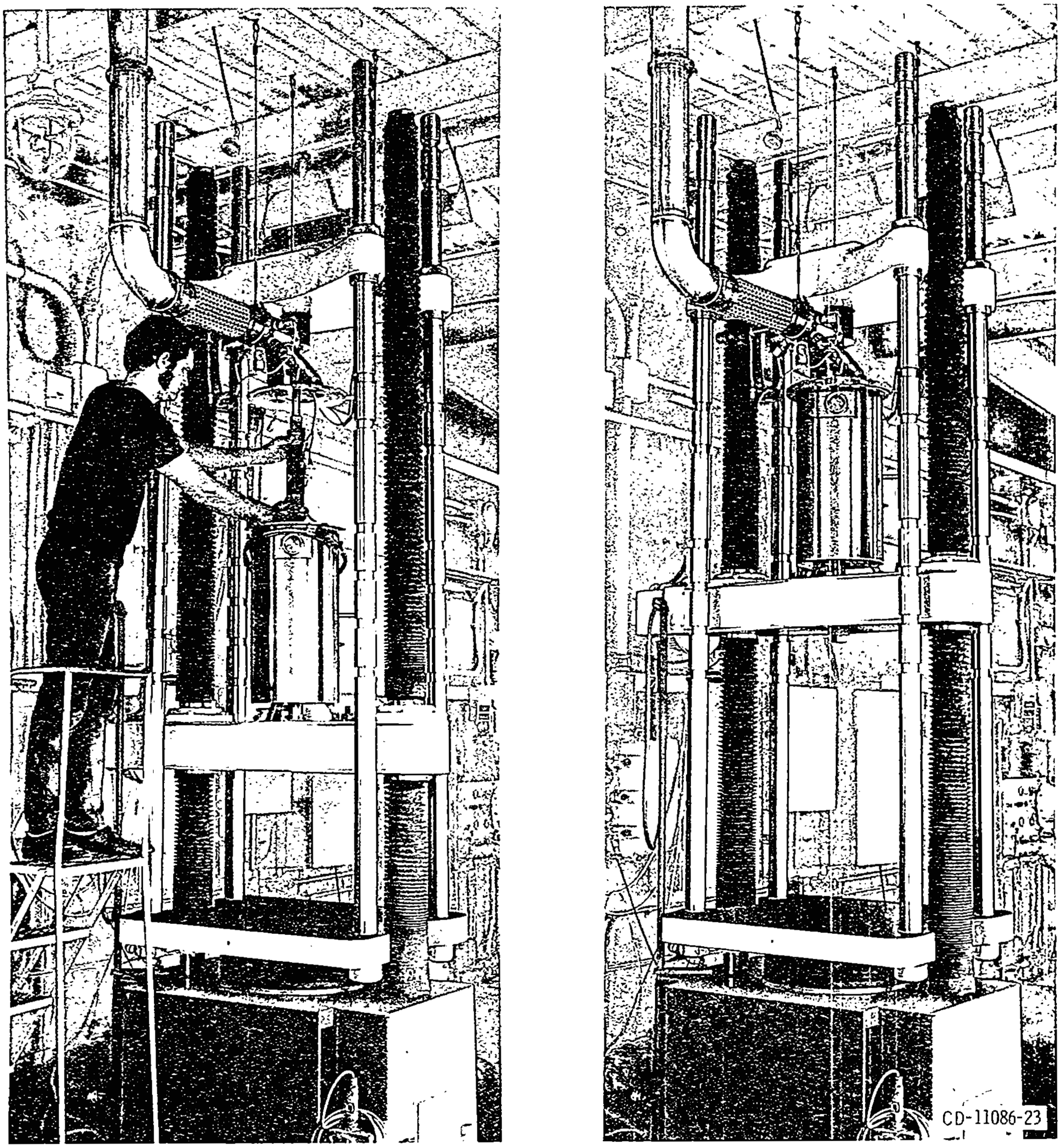

(a) Cryostat lowered.

(b) Cryostat raised.

Figure 3. - Testing machine and cryostat.

the specimen failed. First, a piece of aluminum foil was bonded to the specimen with the 12-millimeter (0.5-in.) section over the crack left unbonded. The strain gage was then bonded to the foil.

Specimens were loaded in a 534 000-newton (120 000-lb) capacity, hydraulically actuated universal testing machine. For the smooth property tests the environments were room temperature air, 77 K liquid nitrogen or 20 K liquid hydrogen. Cracked specimen tests were conducted in 20 K liquid hydrogen. A closed cryostat was used to contain the cryogenic fluids. The testing machine and cryostat are shown in figure 3.

RESULTS AND DISCUSSION

All the experimental data are presented in table I to VI. Some of the data are also shown graphically in the sections that follow.

Comparison of Fracture Strength of Through and Surface Cracks

It has been suggested that a surface-cracked specimen could fail at a lower stress than a through-cracked specimen having a crack the same length. It has been postulated that this could happen because surface-crack stress intensities are in general governed by plane strain conditions while those of through cracks are governed by plane stress conditions. However, in order for this to occur, surface-crack toughness would have to be less than through-crack toughness by a sufficient amount. To investigate this possibility, through-cracked and surface-cracked specimens were tested, and the results compared as shown in figure 4. Two specimen widths were tested to see if any width effect was present.

In figure 4(a), results from tests of the 1.5-millimeter-thick sheet are given for specimens fatigue cracked in tension-tension. Close to each surface-cracked-specimen data point, the crack depth to sheet thickness ratio a/t is given. Using equation (5), curves of predicted failure stresses are drawn on the figure for K_{cn} = 68 kilonewtons per (centimeter)$^{3/2}$ (62 ksi $\sqrt{\text{in.}}$). This value of K_{cn} is the average value obtained from the through-cracked specimen tests plotted on the figure and is slightly lower than the average value obtained from 76.2-millimeter-wide specimens.

Because the crack depth to crack length ratio $a/2c$ was fixed by the method used to produce cracks, surface cracks grew deeper as they grew longer. The longest cracks were also the deepest cracks. Four of the deepest surface-cracked specimens failed at stresses lower than those indicated for through-cracked specimens. However, some surface-cracked specimens just as deep or deeper than these four failed above the

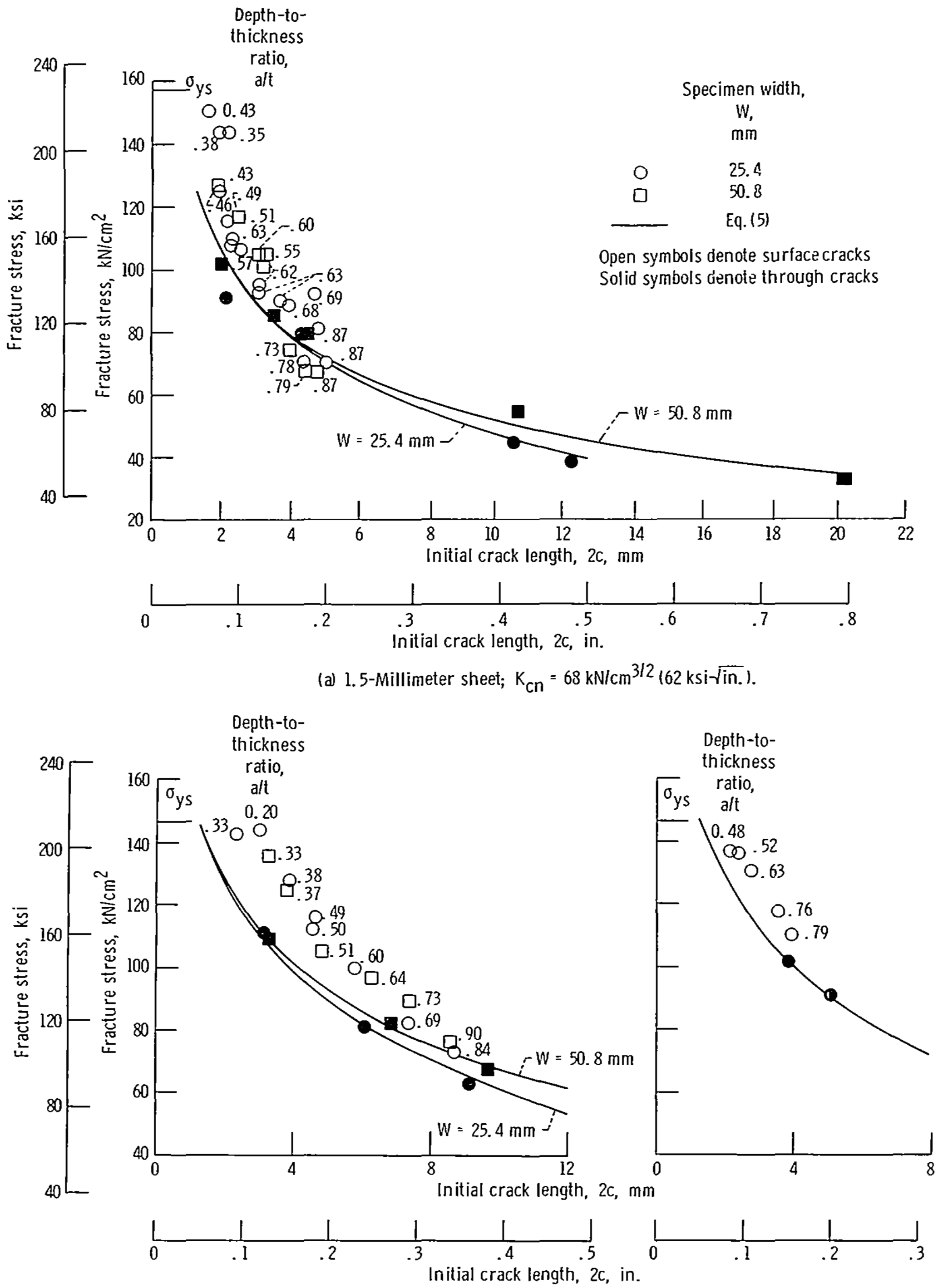

(a) 1.5-Millimeter sheet; K_{cn} = 68 kN/cm$^{3/2}$ (62 ksi-$\sqrt{\text{in.}}$).

(b) 2.8-Millimeter sheet; K_{cn} = 92 kN/cm$^{3/2}$ (84 ksi-$\sqrt{\text{in.}}$).

(c) 1.5-Millimeter sheet reduced from 2.8 millimeter sheet; K_{cn} = 94 kN/cm$^{3/2}$ (86 ksi-$\sqrt{\text{in.}}$).

Figure 4. - Effect of initial crack length on fracture stress of Ti-5Al-2.5Sn ELI at 20 K.

through-cracked specimen line. Because of the scatter in the data, it is not clear if a surface-cracked specimen could fail at a lower stress than one containing a through crack of the same length.

Results from tests using 2.8-millimeter-thick sheet are shown in figure 4(b). Here, equation (5) is used with K_{cn} = 92 kilonewtons per (centimeter)$^{3/2}$ (84 ksi $\sqrt{\text{in.}}$), the average for through-cracked specimen tests plotted on this figure. This average value of K_{cn} is slightly greater than the average value obtained from 76.2-millimeter-wide specimens. Figure 4(b) shows less scatter in the data, and all surface-cracked specimens failed at stresses above those indicated for through-cracked specimens.

For both sheet thicknesses, there was little or no difference between the results using 25.4-millimeter-wide specimens and those using 50.8-millimeter-wide specimens. It was concluded that 25.4 millimeters was a sufficient specimen width for surface cracks up to about 12 millimeters long.

We initially intended to use the two as rolled sheet thicknesses to determine thickness effects. However, the additional processing required to produce the thinner gage changed the properties. It was decided that the difference in properties was great enough so that results from the two gages could not be directly compared. Therefore, some of the 2.8-millimeter sheet was machined down to 1.5 millimeters. Results of tests using this sheet are shown in figure 4(c). Only 25.4-millimeter-wide surface-cracked specimens were tested. Equation (5) is used with K_{cn} = 94 kilonewtons per (centimeter)$^{3/2}$ (86 ksi $\sqrt{\text{in.}}$), the average of the two through-cracked specimen tests plotted on this figure. This average value of K_{cn} is slightly lower than the average value obtained from 76.2-millimeter-wide specimens. Surface-cracked specimens show no tendency to fail at a lower stress than through-cracked specimens with cracks of the same length.

The conclusion to be drawn from the three sets of data plotted in figure 4 is that it would be unlikely for a surface-cracked specimen to fail at a lower stress than a through-cracked specimen having a crack of the same length. This would be the case at least for a sheet material of the thickness and ductility of the one discussed here. Deep surface cracks approach plane stress conditions as restraint on the crack decreases and significant yielding occurs in the uncracked ligament. Because of this yielding, it is unlikely that the crack could penetrate the back surface before fracture occurred. In a pressure vessel, leak before break would be unlikely.

Factors Influencing Apparent Fracture Toughness

The variation of apparent fracture toughness K_Q with crack depth to specimen thickness ratio a/t is shown in figures 5 and 6. Two methods were used to calculate

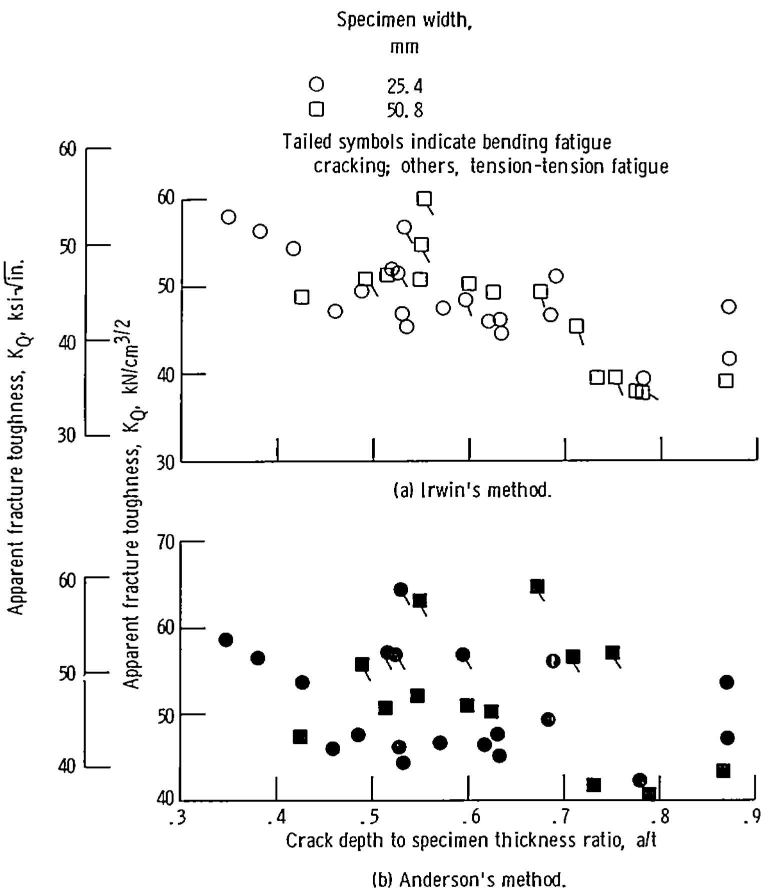

Figure 5. - Variation of apparent fracture toughness with crack depth for 1.5 millimeter Ti-5Al-2.5Sn ELI sheet at 20 K.

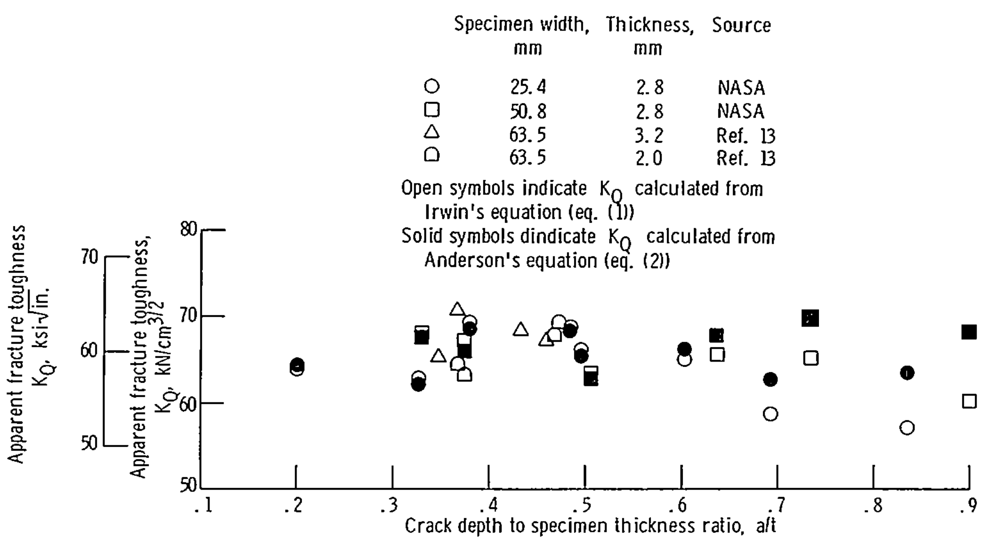

Figure 6. - Variation of apparent fracture toughness with crack depth for 2.0- to 3.2-millimeter Ti-5Al-2.5Sn ELI sheet at 20 K.

toughness, namely, the method of Irwin (eq. (1)) and the method of Anderson (eq. (2)). Initial crack dimensions were used in calculating K_Q.

In figure 5(a), values of K_Q calculated by the Irwin method are plotted for the 1.5-millimeter-thick sheet. The data show a slight reduction in K_Q when a/t exceeds about 0.7. In figure 5(b), K_Q values calculated by the Anderson method are plotted. No reduction in K_Q is apparent for a/t up to 0.9. However, data for smaller values of a/2c (tailed symbols) have all migrated to the top of the scatter band. This would indicate that the Anderson method overcorrects for long, shallow cracks.

There was less scatter in data obtained from the 2.8-millimeter-thick sheet. Values of K_Q obtained using both methods are plotted together in figure 6. For purposes of comparison, data for this alloy from reference 13 are also plotted on this figure The yield stress of the material reported in reference 13 was nearly equal to that of the 2.8-millimeter-thick sheet. Again, Irwin's K_Q drops off slightly when a/t exceeds about 0.7. Anderson's K_Q remains constant for a/t up to 0.9, the deepest crack tested. There is little difference in K_Q calculated by either method for a/t less than 0.6.

The effect of thickness on K_Q is illustrated in figure 7 where Irwin's apparent K_Q is plotted as a function of fracture strength to yield strength ratio. Data obtained from 25.4-millimeter-wide specimens are shown for thicknesses of 1.5 and 2.8 millimeters. The 1.5-millimeter thickness was obtained in one case by rolling and in the second case by machining down the 2.8-millimeter sheet. All three sets of data show K_Q increasing with σ_c/σ_{ys}. The two upper curves show K_Q decreasing as σ_c approaches σ_{ys}. There was about an 8-percent decrease in K_Q when the 2.8-millimeter material was

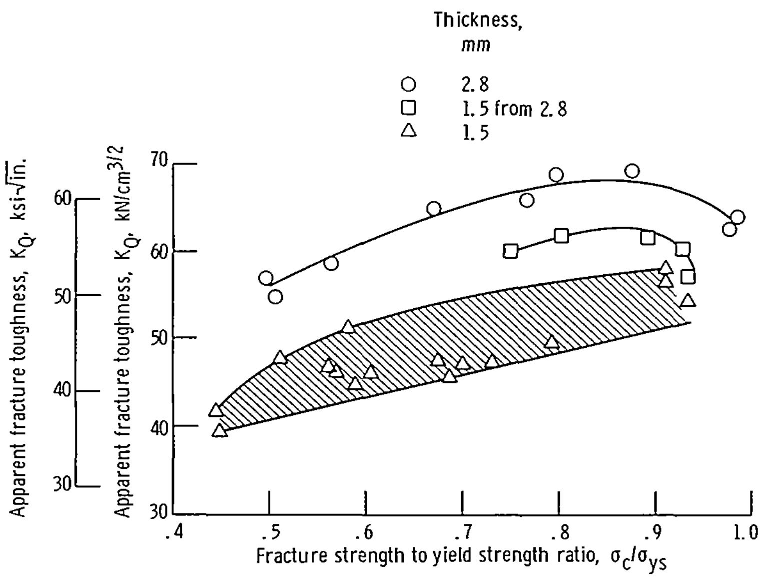

Figure 7. - Comparison of Irwin's apparent fracture toughness for various thicknesses of Ti-5Al-2.5Sn ELI sheet at 20 K. Specimen width, 25.4 millimeters.

machined to 1.5 millimeters. In contrast to this behavior, through crack fracture toughness K_c increased with decreasing thickness. Considering only data from 76.2-millimeter-wide specimens with 25-millimeter-long cracks (table IV), K_{cn} increased from 88 to 101 kilonewtons per (centimeter)$^{3/2}$ (80 to 92 ksi $\sqrt{\text{in.}}$), and K_c increased from 95 to 134 kilonewtons per (centimeter)$^{3/2}$ (86 to 122 ksi $\sqrt{\text{in.}}$) when the sheet thickness was reduced from 2.8 to 1.5 millimeters by machining. The K_Q values of the as-rolled 1.5-millimeter sheet were about 20 percent less than those obtained from the 2.8-millimeter sheet. However, this was both a thickness and a metallurgical effect. The thickness sensitivity exhibited shows that K_Q as determined for the specimens tested in this program is not K_{Ic}.

The fact that K_Q remains relatively constant with crack depth indicates that it can be a useful parameter for the designer. However, the fact that it is thickness dependent (just as is K_c) indicates that it must be determined for each thickness of interest.

Subcritical Growth of Surface Cracks

An effort was made in this program to determine (1) if subcritical growth takes place in surface-cracked specimens as they are loaded monotonically to failure, (2) the extent of this growth if it does occur, and (3) the effect of subcritical crack growth on the proof test logic. It was found that subcritical growth did occur. The cracks grew primarily in the depth direction, with no detectable length growth on the surface. Figure 8 illustrates the extent of growth in two specimens where loading was halted before fracture. The stress achieved before unloading the specimen is given in this figure. Fracturing these specimens at room temperature marked the extent of subcritical growth.

Figure 8(a) shows growth in a 2.8-millimeter-thick specimen. Growth was entirely in the depth direction. In 1.5-millimeter-thick specimens (fig. 8(b)), subsurface length growth as well as depth growth took place. These results are fairly typical of all specimens tested. Subcritical growth took place in steps. This was indicated by the instrumentation as a step increase in strain shown both by the strain gage over the crack and by the one on the surface behind the crack.

To determine the effect of subcritical growth in surface cracks on the proof test logic, some specimens were loaded until the instrumentation indicated that growth had occurred. The specimens were unloaded and reloaded to failure either immediately or after cycling at 75 to 80 percent of the first load for less than 100 cycles. Of the six specimens tested in this manner, two failed during cycling, two failed before reaching the initial load, and two exceeded the initial load. Of the two specimens that failed before reaching the initial load, one failed at a load more than 5 percent below the initial load. Considering the initial load as a proof test, the life of this specimen can be illus-

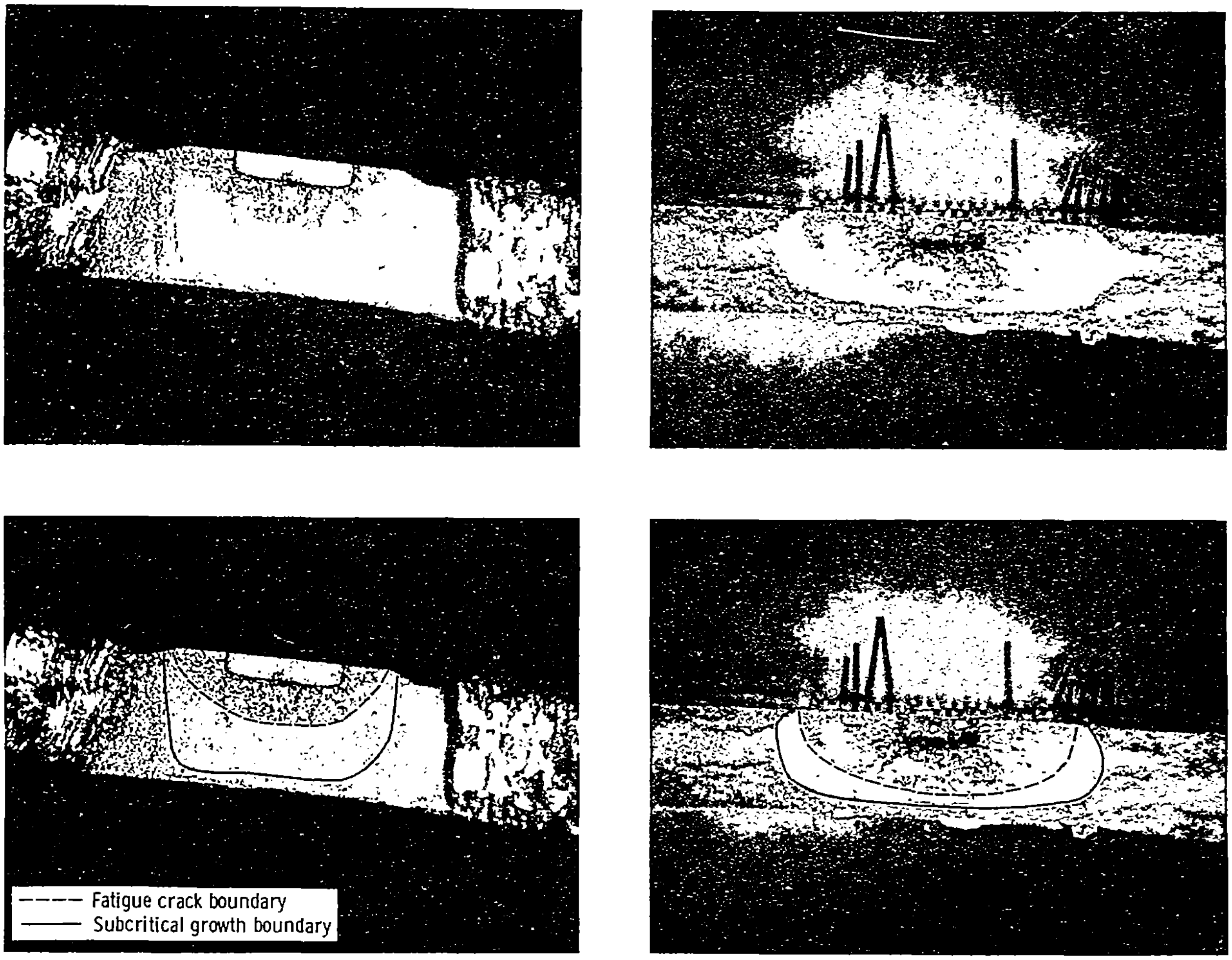

(a) Specimen thickness, 2.8 millimeters; crack depth, 1.5 millimeters; crack length, 4.8 millimeters; gross stress, 105 kilonewtons per square centimeter.

(b) Specimen thickness, 1.5 millimeters; crack depth, 1.3 millimeters; crack length, 4.3 millimeters; gross stress, 75 kilonewtons per square centimeter.

Figure 8. - Subcritical crack growth in Ti-5Al-2.5Sn ELI sheet at 20 K.

trated schematically as shown in figure 9. The fracture surface showed no evidence that growth took place during the cyclic loading. If that was the case, the growth that took place during proofing was sufficient to cause failure before operating load was achieved.

It is the purpose here only to show that the behavior illustrated in figure 9 is possible. Three out of four specimens tested did not behave in this manner. Comparing the proof stress and crack size with the data plotted on figure 4(b) shows that the proofed specimen was at the point of incipient failure. It was fortuitous that failure did not occur at that point. However, the chance of failure can be further reduced by increasing the difference between proof and operating load and by instrumenting the structure to detect crack growth during proof testing.

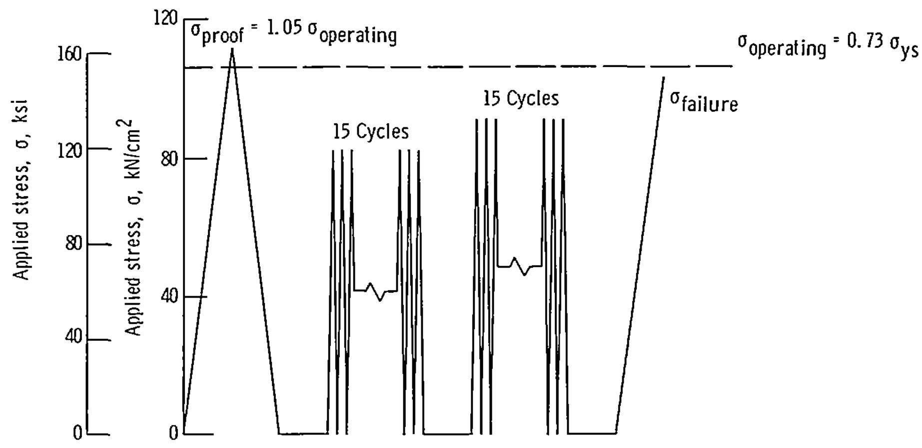

Figure 9. - Load history of surface-cracked titanium specimen at 20 K. Specimen thickness, 2.88 millimeters; crack depth-to-specimen thickness ratio, 0.53; crack depth-to-crack length ratio, 0.31.

Toughness In and Near Welds

Because welds are the most likely place for flaws to occur, the behavior of welds of Ti-5Al-2.5Sn ELI in the presence of cracks was investigated. Through and surface cracks were placed in the center of the weld, in the fusion line, and in the heat affected zone. Welds were made both in a chamber and in open air. Specimens were then tested and the results compared.

Weld test results are shown in figure 10. Specimens 76.2 millimeters wide containing 25-millimeter-long through cracks were used to determine K_c and K_{cn}. Specimens 25.4 and 50.8 millimeters wide containing surface cracks were used to determine K_Q by the Irwin method. Average values of K_c, K_{cn}, and K_Q from the parent metal are shown in the figure for reference.

Results for 1.5-millimeter-thick sheet are shown in figure 10(a). In the weld, K_c, and K_{cn} were substantially greater than parent metal values. This indicates an increased resistance to crack growth in the length direction. The K_Q values obtained in the weld metal were close to parent metal results. As the toughness measurement location varied from the weld zone through the heat affected zone, toughness values approached those obtained in parent metal. In most cases little difference was found between chamber and open air weld results. In general, the chamber welds exhibited slightly greater toughness.

Results for the 2.8-millimeter-thick sheet are shown in figure 10(b). Here the toughness in the weld metal was less than that of the parent metal. A significant reduc-

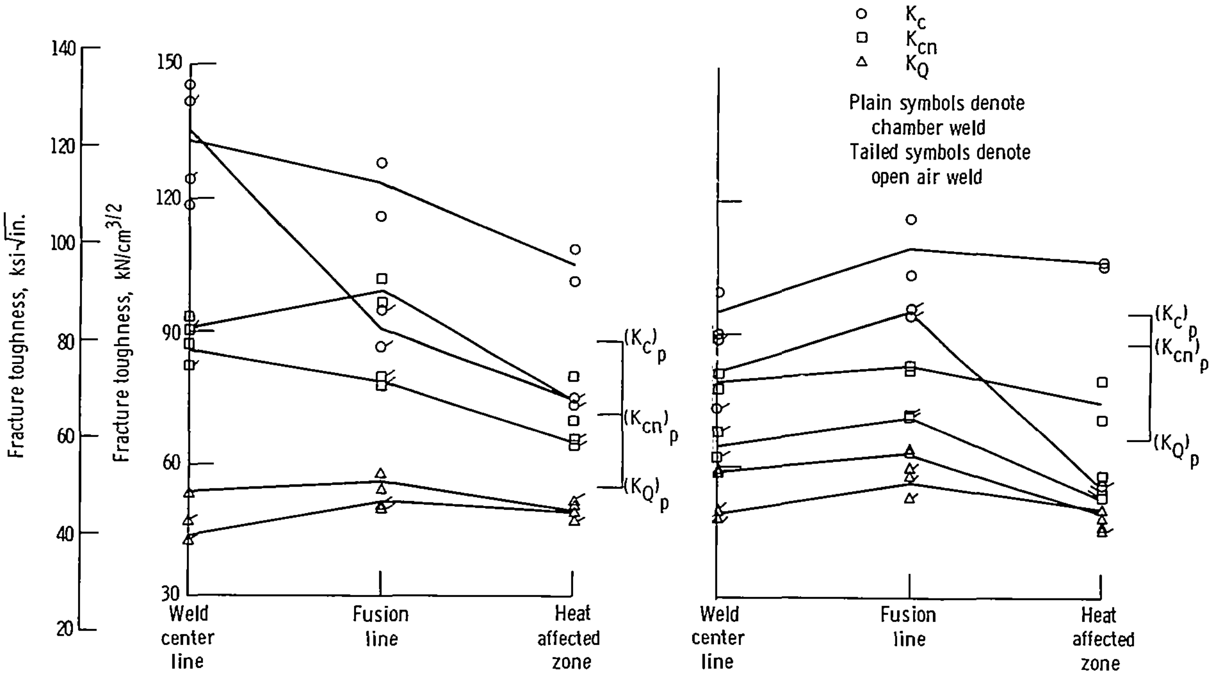

(a) 1.5-Millimeter sheet.

(b) 2.8-Millimeter sheet.

Figure 10. - Comparison of fracture toughness at 20 K for chamber and open air weleded Ti-5Al-2.5Sn ELI sheet.

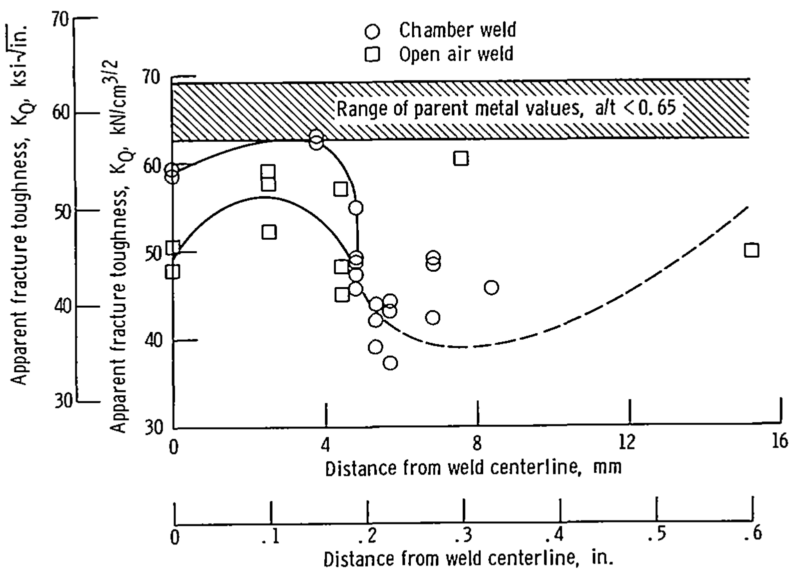

Figure 11. - Fracture toughness in weld region for 2.8-millimeter Ti-5Al-2.5 Sn ELI sheet at 20 K.

tion in toughness was found in the heat affected zone. The chamber welds consistantly exhibited greater toughness than the open air welds.

To further investigate the reduction of toughness in the heat affected zone, surface-cracked specimens were tested with cracks placed as far as 15 millimeters (0.6 in.) from the center of the weld. Results of these tests are shown in figure 11. Toughness obtained from the specimen tested with the crack furthest from the weld was still below parent-metal values. There are several possible causes for this loss of toughness. Heat from the welding process, heat from stress relief, or residual stress may be the cause. However, it is unlikely that sufficient heat from welding penetrated as far as 15 millimeters. In reference 7, it is reported that residual stress had no effect on toughness.

The most likely cause for the loss of toughness was the stress relief treatment. However, this is by no means certain because no indication was found in the literature concerning the possibility of the effect observed, and no deleterious effect from stress relieving was observed in the 1.5-millimeter-thick material. No difference in microstructure was found between the stress-relieved and as-received parent metal.

Structure of Parent and Weld Metal

Photomacrographs of welds of the two sheet thicknesses and two weld methods are shown in figure 12. Comparing figures 12(a) and (c) with 12(b) and (d) shows that the

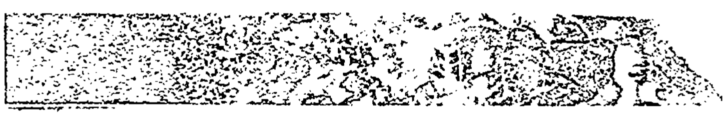

(a) 1.5-Millimeter sheet; chamber weld.

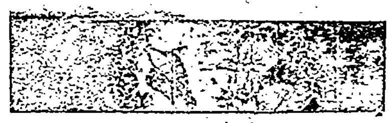

(b) 1.5-Millimeter sheet; open air weld.

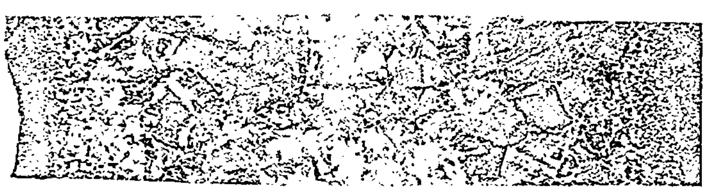

(c) 2.8-Millimeter sheet; chamber weld.

(d) 2.8-Millimeter sheet; open air weld.

Figure 12. - Ti-5Al-2.5Sn ELI weld macrostructure. X8.

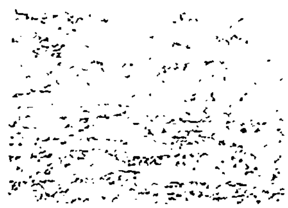

(a) 1.5-Millimeter sheet. (b) 2.8-Millimeter sheet.

Figure 13. - Microstructure of as-received Ti-5Al-2.5Sn ELI sheet. X100.

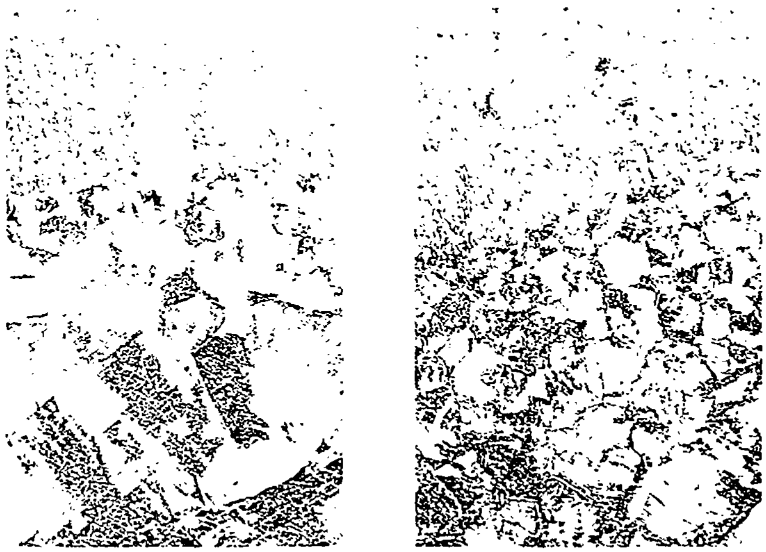

(a) 1.5-Millimeter sheet. (b) 2.8-Millimeter sheet.

Figure 14. - Microstructure of transition region of Ti-5Al-2.5Sn ELI welds. X100.

weld-zone width of the chamber welds was about twice that of the open air welds. The structures are typical for the material and weld techniques used. The weld center is a very large grained acicular alpha structure. Moving out from the weld center, a transition zone is encountered followed by the unaffected base metal. The transition from melted metal to unmelted metal is undetectable metallographically.

Figure 13 shows the as-received microstructure of the two sheet gages. The 1.5-millimeter-sheet (fig. 13(a)) exhibited an elongated alpha structure indicative, perhaps, of an incomplete annealing treatment. The 2.8-millimeter sheet (fig. 13(b)) exhibited the typical equiaxed alpha structure. Figure 14 shows the transition from heat affected to unaffected metal.

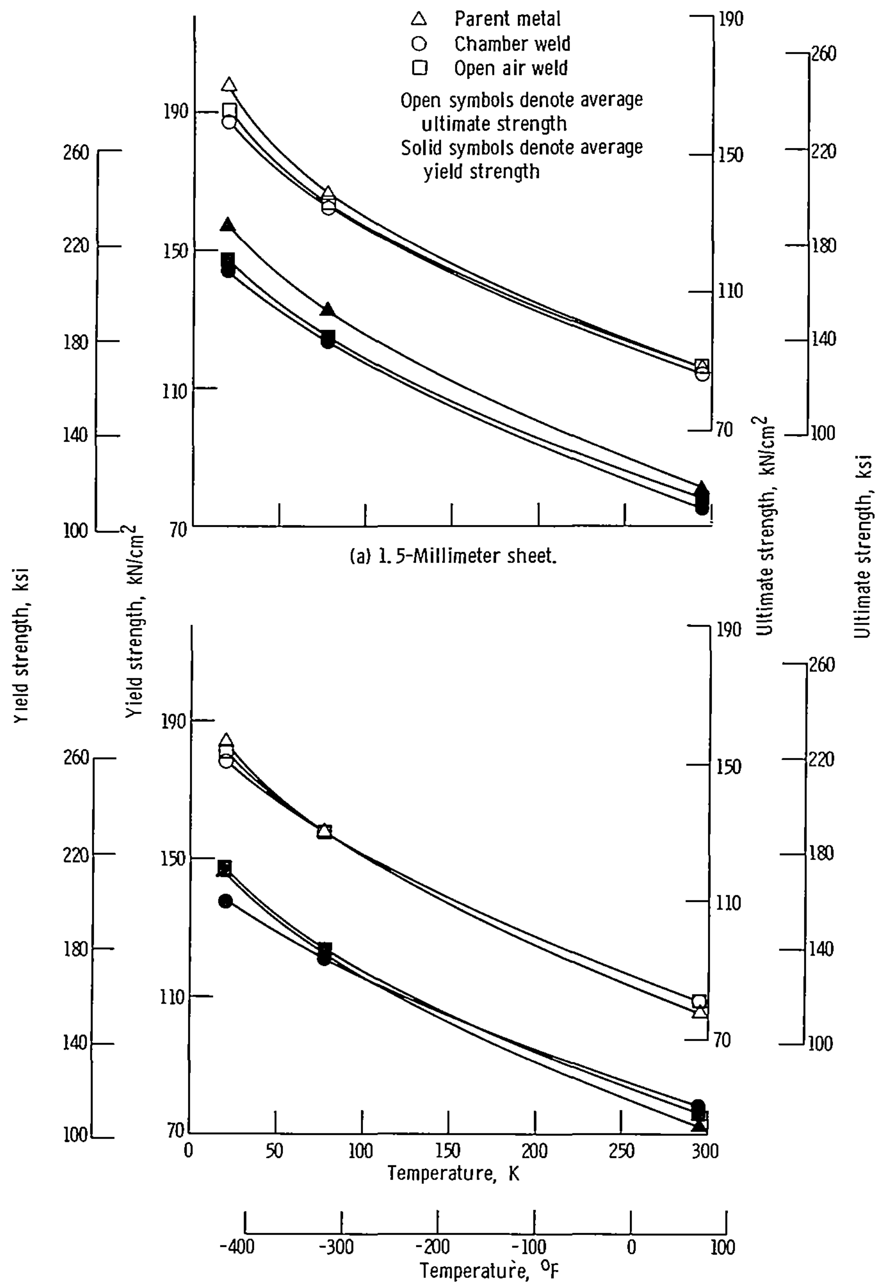

(b) 2.8-Millimeter sheet.

Figure 15. - Strength of Ti-5Al-2.5Sn ELI parent and weld metal.

Smooth Properties of Parent and Weld Metal

Yield and ultimate strength were determined for the parent metal and for welds produced by the two weld processes. Tests were conducted at 20 and 77 K and at room temperature. Figure 15 shows the results of these tests. In the 1.5-millimeter sheet (fig. 15(a)), the parent metal exhibited greater yield and ultimate strength than the welds. The difference in strength between chamber and open air welds was very small, with the open air weld slightly stronger. Weld efficiencies were high and ranged from about 94 percent at 20 K to close to 100 percent at room temperature.

Results were mixed with the 2.8-millimeter sheet yield strength (fig. 15(b)). At room temperature the chamber weld exhibited the greatest yield strength, at 20 K it had the lowest. Weld efficiencies again were high and ranged from about 97 percent at 20 K to 100 percent at 77 K and 104 percent at room temperature.

CONCLUDING REMARKS

The results of this investigation of the behavior at 20 K of Ti-5Al-2.5Sn ELI parent and weld metal when through and surface cracks are present can be summarized as follows:

1. For the material and sheet thicknesses investigated here, it is unlikely that a structure containing a surface crack will fail at a lower stress than one having a through crack of the same length. It is also unlikely that leak before burst behavior will occur.

2. Relatively constant values of apparent surface-crack fracture toughness K_Q were calculated by the Anderson method for cracks up to 90 percent of sheet thickness. However, there was evidence that the Anderson method overcorrected for surface cracks with small depth to length ratios.

3. Apparent toughness K_Q varied with sheet thickness, and therefore cannot be construed to be K_{Ic}. If used as a design parameter, K_Q can only be used for the sheet thickness from which it was obtained.

4. Significant subcritical crack growth took place in the depth direction of the surface cracked specimens during monotonic loading to failure. One out of four specimens subjected to a simulated proof load subsequently did not reach its corresponding operating load because of crack growth during proofing.

5. The toughness levels obtained in and near the welds in most cases compared favorably with those of the parent metal. However, a significant reduction in toughness in the heat affected zone of the 2.8-millimeter sheet was encountered.

6. Weld efficiencies were high. They ranged from 94 percent at 20 K to over 100 percent at room temperature.

Lewis Research Center,
National Aeronautics and Space Administration,
Cleveland, Ohio, August 5, 1971,
124-08.

REFERENCES

1. Irwin, G. R.: Crack-Extension Force for a Part-Through Crack in a Plate. J. Appl. Mech., vol. 29, no. 4, Dec. 1962, pp. 651-654.
2. Brown, William F., Jr.; and Srawley, John E.: Plane Strain Crack Toughness Testing of High Strength Metallic Maretials. Spec. Tech. Publ. No. 410, ASTM, 1967, pp. 25-26.
3. Anderson, Robert B.; and Sullivan, Timothy L.: Fracture Mechanics of Through-Cracked Cylindrical Pressure Vessels. NASA TN D-3252, 1966.
4. Sullivan, Timothy L.: Uniaxial and Biaxial Fracture Toughness of Extra-Low Interstitial 5Al-2.5Sn Titanium Alloy Sheet at 20° K. NASA TN D-4016, 1967.
5. Sullivan, Timothy L.: Texture Strengthening and Fracture Toughness of Titanium Alloy Sheet at Room and Cryogenic Temperatures. NASA TN D-4444, 1968.
6. Sullivan, Timothy L.; and Pierce, William S.: Effect of Radius on Bulging and Fracture of Through-Cracked Cylindrical Pressure Vessels at Cryogenic Temperatures. NASA TN D-4951, 1968.
7. Robelotto, R.; Lambase, J. M.; and Toy, A.: Residual Stresses in Welded Titanium and Their Effects on Mechanical Behavior. Welding J. Res. Suppl., vol. 47, no. 7, July 1968, pp. 289-s to 298-s.
8. Pyle, Richard; Schillinger, David E.; Carman, Carl M.: Plane Strain Fracture Toughness and Mechanical Properties of 2219-T87 Aluminum and 5Al-2.5Sn ELI Titanium Alloy Weldments and One Inch Thick 5Al-2.5Sn ELI Titanium Alloy Plate. Rep. FA-R-1897, Frankford Arsenal. (NASA CR-72154), Sept. 1968.
9. Anderson, Robert B.; Holms, Arthur G.; and Orange, Thomas W.: Stress Intensity Magnification for Deep Surface Cracks in Sheets and Plates. NASA TN D-6054, 1970.

10. Kobayashi, A. S.; and Moss, W. L.: Stress Intensity Magnification Factors for Surface-Flawed Tension Plate and Notched Round Tension Bar. Fracture; Proceedings of the Second International Conference on Fracture, Brighton, England, Apr. 13-18, 1969, pp. 31-45.

11. ASTM Special Committee on Fracture Toughness Testing of High-Strength Metallic Materials: Fracture Testing of High-Strength Sheet Materials. Part I. ASTM Bull. No. 243, Jan. 1960, pp. 29-40.

12. Sullivan, Timothy L.; and Orange, Thomas W.: Continuity Gage Measurement of Crack Growth on Flat and Curved Surfaces at Cryogenic Temperatures. NASA TN D-3747, 1966.

13. Hall, L. R.; and Finger, R. W.: Investigation of Flaw Geometry and Loading Effects on Plane Strain Fracture in Metallic Structures. NASA CR-72659, The Boeing Co., 1971.

TABLE I. - RESULTS OF SURFACE-CRACKED SPECIMEN TESTS OF 1.5-MILLIMETER (0.06-IN.) ROLLED SHEET

Crack location and weld type (a)	Specimen width		Specimen thickness, t		Crack depth, a		Crack length, 2c		Fracture stress		Irwin's toughness (eq. (1)), K_Q		Anderson's toughness (eq. (2)), K_Q		Depth-to-thickness ratio, a/t	Depth to length ratio, a/2c
	mm	in	mm	in.	mm	in.	mm	in.	kN/cm^2	ksi	kN/cm$^{3/2}$	ksi$\sqrt{\text{in.}}$	kN/cm$^{3/2}$	ksi$\sqrt{\text{in.}}$		
P	25.4	1.0	1.65	0.0650	1.03	0.041	3.73	0.147	90	130	46.1	41.9	47.6	43.3	0.63	0.28
			1.63	.0642	1.42	.056	5.08	.200	70	102	41.6	37.8	47.2	42.9	.87	.28
			1.63	0640	1.27	.050	4.39	.173	70	102	39.3	35.7	42.4	38.5	.78	.29
			1.65	.0648	.94	.037	2.59	.102	106	154	47.5	43.2	46.6	42.4	.57	.36
			1.60	.0631	.69	.027	1.65	.065	147	213	54.4	49.5	53.7	48.8	.43	.42
			1.62	.0636	.79	.031	1.96	.077	125	181	49.5	45.0	47.6	43.3	.49	.40
			1.64	.0647	1.02	.040	3.12	.123	95	138	46.0	41.8	46.3	42.1	.62	.33
			1.60	.0630	.56	022	2.26	.089	143	208	58.1	52.8	58.7	53.4	.35	.25
			1.60	.0628	.61	.024	1.98	.078	143	208	56.5	51.4	56.4	51.3	.38	.31
			1.63	.0643	1.42	.056	4.88	192	81	117	47.5	43.2	53.6	48.7	.87	.29
			1.62	.0638	1.12	.044	4.75	.187	92	133	51.2	46.5	56.1	51.0	.69	.24
			1.60	0630	.84	.033	7.26	.286	94	137	51.6	46.9	57.0	51.8	.52	.12
			1.62	.0639	.84	.033	7.62	.300	94	137	51.9	47.2	57.1	51.9	.52	.11
			1.58	.0622	.94	.037	9.98	.393	83	120	48.4	44.0	56.8	51.6	.60	.09
			1.63	.0640	.86	.034	9.93	391	99	144	56.8	51.6	64.4	58.5	.53	.09
			1.57	.0618	.84	.033	2.29	.090	107	156	45.4	41.3	44.3	40.3	.53	.37
			1.60	.0631	.74	.029	2.18	.086	115	167	47.2	42.9	46.0	41.8	.46	.34
			1.54	.0605	.81	.032	2.36	.093	110	159	46.9	42.6	46.1	41.9	.53	.34
			1.61	.0632	1.02	.040	3.12	.123	92	134	44.6	40.5	45.1	41.0	.63	.33
			1.60	.0629	1.09	.043	3.99	.157	88	128	46.6	42.4	49.3	44.8	.68	.27
	50.8	2.0	1.64	0.0646	1.42	0.056	4.83	0.190	67	97	38.9	35.4	43.3	39.4	0.87	0.30
			1.58	.0621	.86	.034	3.35	.132	105	152	50.8	46.2	52.0	47.3	.55	.26
			1.64	.0646	1.30	.051	4.44	.175	68	98	37.8	34.4	40.8	37.1	.79	.29
			1.60	.0628	1.17	.046	4.01	.158	74	107	39.5	35.9	41.8	38.0	.73	.29
			1.61	.0635	.69	.027	1.90	.075	126	183	49.0	44.5	47.4	43.1	.43	.36
			1.63	.0643	.84	.033	2.51	.099	116	169	51.4	46.7	50.6	46.0	.51	.33
			1.61	0635	.97	.038	3.10	.122	105	152	50.4	45.8	51.0	46.4	.60	.31
			1.63	.0641	1.02	.040	3.25	128	101	146	49.4	44.9	50.3	45.7	.62	.31
			1.60	.0631	.79	031	7.54	.297	95	138	50.9	46.3	55.7	50.6	.49	.10
			1.61	0633	1.14	045	8.92	.351	73	106	45.4	41.3	56.4	51.3	.71	.13
			1.62	.0637	.89	.035	10.13	.399	95	138	54.9	49.9	63.1	57.4	.55	.09

[a] P denotes parent metal; W, weld centerline, FL, fusion line, HAZ, heat affected zone, C, chamber weld, OA, open air weld.

[b] Solution did not converge.

[c] Plastic zone penetrated back surface.

TABLE I. - Concluded. RESULTS OF SURFACE-CRACKED SPECIMEN TESTS OF 1.5-MILLIMETER (0.06-IN.) ROLLED SHEET

Crack location and weld type (a)	Specimen width		Specimen thickness, t		Crack depth, a		Crack length, 2c		Fracture stress		Irwin's toughness (eq. (1)), K_Q		Anderson's toughness (eq. (2)), K_Q		Depth-to-thickness ratio, a/t	Depth to length ratio, a/2c
	mm	in.	mm	in.	mm	in.	mm	in.	kN/cm^2	ksi	$kN/cm^{3/2}$	$ksi\sqrt{in.}$	$kN/cm^{3/2}$	$ksi\sqrt{in.}$		
P	50.8	2.0	1.61	0.0634	0.89	0.035	9.88	0.389	103	150	60.1	54.6	(b)	(b)	0.55	0.09
			1.62	.0639	1.09	.043	14.99	.590	77	112	49.4	44.9	64.7	58.8	.67	.07
			1.59	.0627	1.24	.049	20.83	.820	56	81	37.8	34.4	(c)	(c)	.78	.06
			1.62	.0638	1.22	.048	19.86	.782	59	85	39.5	35.9	57.0	51.8	.75	.06
W, C	25.4	1.0	1.62	0.0638	1.07	0.042	2.08	0.082	117	170	48.2	43.8	46.0	41.8	0.66	0.51
			1.60	.0628	.99	.039	2.24	.088	131	190	56.3	51.2	(b)	(b)	.62	.44
			1.58	.0622	1.32	.052	3.18	.125	96	140	48.4	44.0	49.2	44.7	.84	.42
			1.59	.0626	.79	.031	1.78	.070	133	193	51.2	46.5	50.5	45.9	.50	.44
			1.62	.0636	1.22	.048	3.07	.121	114	165	56.5	51.4	59.3	53.9	.76	.40
	50.8	2.0	1.62	0.0637	1.40	0.055	4.17	0.164	93	135	52.4	47.6	57.5	52.3	0.86	0.34
			1.61	.0635	.97	.038	2.31	.091	130	188	56.5	51.4	59.0	53.6	.60	.42
			1.60	.0630	.94	.037	2.03	.080	127	184	51.9	47.2	51.0	46.4	.59	.46
W, OA	25.4	1.0	1.51	0.0596	0.89	0.035	2.11	0.083	103	150	42.4	38.5	40.8	37.1	0.59	0.42
			1.57	.0619	1.32	.052	2.41	.095	97	141	42.4	38.5	40.2	36.5	.84	.55
			1.55	.0610	.89	.035	2.41	.095	107	156	46.8	42.5	46.1	41.9	.57	.37
			1.55	.0612	.81	.032	1.93	.076	108	157	42.5	38.6	40.7	37.0	.52	.42
FL, C	25.4	1.0	1.58	0.0624	0.79	0.031	1.75	0.069	141	205	54.2	49.3	(c)	(c)	0.50	0.45
			1.59	.0625	1.14	.045	2.82	.111	120	174	57.4	52.2	61.8	56.2	.71	.41
FL, OA	25.4	1.0	1.54	0.0606	0.69	0.027	1.60	0.063	136	198	49.7	45.2	48.7	44.3	0.45	0.43
			1.56	.0615	.76	.030	2.69	.106	112	163	49.9	45.4	50.2	45.6	.49	.28
			1.57	.0620	1.02	.040	2.56	.101	136	198	62.9	57.2	(c)	(c)	.65	.40
			1.54	.0608	.91	.036	2.36	.093	125	182	54.8	49.8	55.3	50.3	.59	.39
HAZ, C	25.4	1.0	1.58	0.0622	0.86	0.034	1.98	0.078	121	176	48.8	44.4	47.3	43.0	0.55	0.44
			1.53	.0604	.99	.039	2.95	.116	103	150	49.3	44.8	49.9	45.4	.65	.34
HAZ, OA	25.4	1.0	1.57	0.0617	0.76	0.030	1.98	0.078	123	179	49.4	44.9	48.2	43.8	0.49	0.39
			1.55	.0612	.81	.032	2.72	.107	113	164	51.2	46.5	51.6	46.9	.53	.30
			1.56	.0615	.94	.037	2.56	.101	104	151	46.6	42.4	46.1	41.9	.60	.37
			1.57	.0618	.86	.034	2.54	.100	112	163	50.1	45.5	49.8	45.3	.55	.34

[a]P denotes parent metal; W, weld centerline; FL, fusion line; HAZ, heat affected zone; C, chamber weld; OA, open air weld.
[b]Solution did not converge.
[c]Plastic zone penetrated back surface.

TABLE II. - RESULTS OF SURFACE-CRACKED SPECIMEN TESTS OF 2.8-MILLIMETER (0.11-IN.) ROLLED SHEET AND OF 1.5-MILLIMETER (0.06-IN.) MACHINED SHEET

Crack location and weld type (a)	Specimen width		Specimen thickness, t		Crack depth, a		Crack length, 2c		Fracture stress		Irwin's toughness (eq. (1)), K_Q		Anderson's toughness (eq. (2)), K_Q		Depth-to-thickness ratio, a/t	Depth to length ratio, a/2c
	mm	in.	mm	in.	mm	in.	mm	in.	kN/cm^2	ksi	kN/cm$^{3/2}$	ksi $\sqrt{\text{in.}}$	kN/cm$^{3/2}$	ksi $\sqrt{\text{in.}}$		
P	25.4	1.0	2.94	0.1157	0.58	0.023	3.00	0.118	143	208	64.0	58.2	64.1	58.3	0.20	0.20
			2.87	.1129	1.42	.056	4.55	.179	112	162	65.9	59.9	65.3	59.4	.50	.31
			2.86	.1128	1.73	.068	5.77	.227	99	144	64.9	59.0	66.2	60.2	.60	.30
			2.82	.1111	1.96	.077	7.37	.290	82	119	58.5	53.2	62.5	56.8	.69	.27
			2.88	.1133	1.09	.043	3.88	.153	127	185	69.2	62.9	68.8	62.5	.38	.28
			2.95	.1161	2.46	.097	8.69	.342	72	105	56.9	51.7	63.2	57.5	.83	.28
			2.88	.1132	.94	.037	2.34	.092	142	206	62.7	57.0	62.3	56.6	.33	.40
			2.88	.1135	1.40	.055	4.65	.183	116	168	68.8	62.5	68.9	62.6	.49	.30
	50.8	2.0	2.85	0.1122	0.94	0.037	3.28	0.129	135	196	67.9	61.7	67.5	61.4	0.33	0.29
			2.93	.1152	1.09	.043	3.81	.150	124	180[b]	67.0	60.9	65.8	59.8	.37	.29
			2.91	.1144	1.47	.058	4.80	.189	105	152[b]	63.2	57.5	62.6	56.9	.51	.31
			2.91	.1147	1.85	.073	6.27	.247	96	140	65.4	59.5	67.6	61.5	.64	.30
			2.90	.1143	2.13	.084	7.39	.291	89	129	65.0	59.1	69.6	63.3	.73	.29
			2.84	.1119	2.56	.101	8.56	.337	76	110	59.8	54.4	68.0	61.8	.90	.30
W, C	25.4	1.0	2.85	0.1121	0.99	0.039	3.45	0.136	115	167	58.7	53.4	57.6	52.4	0.35	0.29
			2.92	.1150	1.96	.077	5.51	.217	91	132	59.4	54.0	59.7	54.3	.67	.36
W, OA	25.1	1.0	2.80	0.1101	1.52	0.060	3.63	0.143	94	137	50.5	45.9	48.3	43.9	0.55	0.42
			2.90	.1143	2.39	.094	5.26	.207	75	109	48.0	43.6	47.1	42.8	.82	.45
FL, C	25.1	1.0	2.84	0.1120	1.24	0.049	3.45	0.136	118	172	62.5	56.8	61.3	55.7	0.44	0.36
			2.84	.1120	2.41	.095	5.72	.225	94	136	63.1	57.4	64.4	58.5	.85	.42
FL, OA	25.1	1.0	2.91	0.1146	1.47	0.058	3.07	0.121	116	168	57.8	52.5	54.4	49.5	0.51	0.48
			2.87	.1129	2.44	.096	5.11	.201	83	120	52.4	47.6	51.0	46.4	.85	.48
			2.85	.1122	1.93	.076	4.65	.183	98	142	59.3	53.9	58.1	52.8	.68	.42
HAZ, C	25.1	1.0	2.87	0.1129	2.21	0.087	5.33	0.210	76	110	48.8	44.4	48.5	44.1	0.77	0.41
			2.77	.1092	1.17	.046	3.86	.152	89	129	47.4	43.1	46.2	42.0	.42	.30
			2.87	.1129	2.46	.097	6.20	.244	66	96	45.8	41.6	46.8	42.5	.86	.40
			2.85	.1123	1.70	.067	4.83	.190	70	101	42.0	38.2	41.6	37.8	.60	.39
			2.85	.1121	1.63	.064	4.90	.193	73	106	44.2	40.2	43.9	39.9	.57	.33
			2.87	.1130	1.45	.057	4.98	.196	81	118	48.5	44.1	48.4	44.0	.50	.29

[a]P denotes parent metal; W, weld centerline; FL, fusion line; HAZ, heat affected zone; C, chamber weld; OA, open air weld.

[b]Failed in grip.

[c]Machined from 2.8-millimeter (0.11-in.) sheet.

[d]Plastic zone penetrated back surface.

TABLE II. - Concluded. RESULTS OF SURFACE-CRACKED SPECIMEN TESTS OF 2.8-MILLIMETER (0.11-IN.) ROLLED SHEET AND OF 1.5-MILLIMETER (0.06-IN.) MACHINED SHEET

Crack location and weld type (a)	Specimen width		Specimen thickness, t		Crack depth, a		Crack length, 2c		Fracture stress		Irwin's toughness (eq. (1)), K_Q		Anderson's toughness (eq. (2)), K_Q		Depth-to-thickness ratio, a/t	Depth to length ratio, a/2c
	mm	in.	mm	in.	mm	in.	mm	in.	kN/cm^2	ksi	$kN/cm^{3/2}$	ksi $\sqrt{in.}$	$kN/cm^{3/2}$	ksi $\sqrt{in.}$		
HAZ, C	50.8	2.0	2.90	0.1140	2.36	0.093	6.40	0.252	70	102	49.1	44.6	50.5	45.9	0.82	0.37
			2.83	.1115	1.96	.077	4.90	.193	88	128	54.9	49.9	54.2	49.3	.69	.40
			2.80	.1102	1.85	.073	6.10	.240	59	86	39.0	35.5	40.2	36.5	.66	.30
			2.88	.1136	1.65	.065	4.80	.189	73	106	43.9	39.9	43.4	39.5	.57	.34
			2.82	.1110	1.70	.067	6.25	.246	56	82	37.1	33.7	38.3	34.8	.60	.27
			2.80	.1101	1.52	.060	4.93	.194	72	104	43.1	39.2	43.0	39.1	.55	.31
			2.82	.1110	1.65	.065	5.69	.224	67	97	42.4	38.5	43.0	39.1	.59	.29
			2.84	.1120	1.45	.057	4.67	.184	83	121	49.1	44.6	48.5	44.1	.51	.31
			2.88	.1136	1.52	.060	4.67	.184	77	112	45.6	41.5	45.1	41.0	.53	.29
HAZ, OA	25.4	1.0	2.88	0.1136	1.17	0.046	3.25	0.128	113	164	57.2	52.0	54.9	49.9	0.41	0.36
			2.90	.1140	1.70	.067	5.46	.215	72	104	45.0	40.9	45.2	41.1	.59	.31
			2.87	.1130	1.65	.065	5.21	.205	78	113	48.2	43.8	48.2	43.8	.58	.32
			2.87	.1131	1.47	.058	4.39	.173	87	126	49.8	45.3	48.8	44.4	.51	.34
			2.87	.1130	1.04	.041	2.69	.106	129	187	60.3	54.8	58.0	52.7	.36	.39
P[c]	25.4	1.0	1.58	0.0624	0.99	0.039	2.77	0.109	130	189	61.6	56.0	(d)	(d)	0.63	0.36
				.0624	.76	.030	2.16	.085	136	198	57.2	52.0			.48	.35
				.0624	1.24	.049	3.94	.155	110	159	60.1	54.6			.79	.32
				.0621	.81	.032	2.46	.097	136	197	60.4	54.9			.52	.33
				.0622	1.19	.047	3.56	.140	117	170	61.8	56.2			.76	.34

[a]P denotes parent metal; W, weld centerline; FL, fusion line; HAZ, heat affected zone; C, chamber weld; OA, open air weld.

[b]Failed in grip.

[c]Machined from 2.8-millimeter (0.11-in.) sheet.

[d]Plastic zone penetrated back surface.

TABLE III. - RESULTS OF THROUGH-CRACKED SPECIMEN TESTS OF 1.5-MILLIMETER (0.06-IN.) ROLLED SHEET

Crack location and weld type (a)	Specimen width		Specimen thickness		Initial crack length		Critical crack length		Fracture stress		Nominal fracture toughness (eq. (5)), K_{cn}		Fracture toughness (eq. (4)), K_c	
	mm	in.	mm	in.	mm	in.	mm	in.	kN/cm^2	ksi	$kN/cm^{3/2}$	ksi $\sqrt{in.}$	$kN/cm^{3/2}$	ksi $\sqrt{in.}$
P	25.4	1.0	1.57	0.0616	2.16	0.085	(b)	(b)	90	131	58	53	(b)	(b)
			1.63	.0640	12.2	.481			38	55	64	58		
			1.62	.0639	4.37	.172			79	115	73	66		
			1.60	.0629	10.5	.414			44	64	66	60		
	50.8	2.0	1.58	0.0624	2.03	.080	(b)	(b)	101	147	65	59	(b)	(b)
			1.60	.0632	3.58	.141			85	123	69	63		
			1.60	.0632	4.55	.179			79	115	73	66		
			1.63	.0640	10.7	.420			54	78	75	68		
			1.60	.0628	20.1	.793			32	47	65	59		
	76.2	3.0	1.63	0.0640	25.1	0.988	35.0	1.38	34	49	73	66	93	85
			1.62	.0639	25.3	.995	33.5	1.32	31	45	67	61	82	75
W, C	76.2	3.0	1.56	0.0616	24.6	0.969	33.8	1.33	43	62	94	85	119	108
			1.62	.0637	26.9	1.060	46.5	1.83	38	55	87	79	146	133
W, OA	76.2	3.0	1.50	0.0589	25.3	0.994	37.8	1.49	41	59	90	82	124	113
			1.54	.0609	24.9	.981	45.7	1.80	38	55	82	75	143	130
FL, C	76.2	3.0	1.58	0.0622	24.5	0.963	33.3	1.31	47	68	102	93	129	117
			1.61	.0633	24.4	.960	31.8	1.25	45	65	96	87	117	106
FL, OA	76.2	3.0	1.54	0.0608	24.3	0.957	31.0	1.22	37	54	79	72	95	86
			1.52	.0600	24.0	.945	28.2	1.11	36	53	78	71	87	79
HAZ, C	76.2	3.0	1.59	0.0626	24.7	0.973	42.4	1.67	32	47	69	63	109	99
			1.60	.0630	24.4	.962	33.8	1.33	37	54	80	73	101	92
HAZ, OA	76.2	3.0	1.53	0.0603	26.2	1.032	31.8	1.25	29	42	65	59	75	68
			1.53	.0603	25.8	1.015	31.0	1.22	30	43	65	59	75	68

[a]P denotes parent metal; W, weld centerline; FL, fusion line; HAZ, heat affected zone; C, chamber weld; OA, open air weld.

[b]Not measured.

TABLE IV. - RESULTS OF THROUGH-CRACKED SPECIMEN TESTS OF 2.8-MILLIMETER (0.11-IN.) ROLLED SHEET AND 1.5-MILLIMETER (0.06-IN.) MACHINED SHEET

Crack location and weld type (a)	Specimen width		Specimen thickness		Initial crack length		Critical crack length		Fracture stress		Nominal fracture toughness (eq. (5)), K_{cn}		Fracture toughness (eq. (4)), K_c	
	mm	in.	mm	in.	mm	in.	mm	in.	kN/cm^2	ksi	$kN/cm^{3/2}$	$ksi\sqrt{in.}$	$kN/cm^{3/2}$	$ksi\sqrt{in.}$
P	25.4	1.0	2.83	0.1115	3.12	0.123	(b)	(b)	111	161	94.6	86	(b)	(b)
			2.86	.1126	6.10	.240	(b)	(b)	81	117	91.3	83	(b)	(b)
			2.87	.1128	9.14	.360	(b)	(b)	62	90	89.1	81	(b)	(b)
	50.8	2.0	2.85	0.1122	3.28	0.129	(b)	(b)	109	158	92.4	84	(b)	(b)
			2.88	.1135	6.83	.269	(b)	(b)	82	119	94.6	86	(b)	(b)
			2.86	.1128	9.68	.381	(b)	(b)	67	97	90.2	82	(b)	(b)
	76.2	3.0	2.94	0.1157	26.7	1.051	29.5	1.16	38	55	86.9	79	93.5	85
			2.95	.1162	25.2	.994	28.2	1.11	40	58	89.1	81	95.7	87
W, C	73.7	2.9	2.76	0.1086	25.3	0.997	33.0	1.30	36	53	81.4	74	99.0	90
			2.81	.1108	24.5	.965	29.7	1.17	36	52	78.1	71	89.1	81
W, OA	76.2	3.0	2.85	0.1122	24.9	0.981	32.0	1.26	28	41	61.6	56	72.6	66
			2.81	.1108	24.3	.955	34.8	1.37	32	46	68.2	62	88.0	80
FL, C	73.7	2.9	2.82	0.1110	24.7	0.972	37.6	1.48	38	55	82.5	75	116.6	106
			2.80	.1102	23.9	.942	32.0	1.26	39	56	83.6	76	103.4	94
FL, OA	76.2	3.0	2.83	0.1116	26.9	1.060	38.4	1.51	31	45	71.5	65	94.6	86
			2.86	.1127	25.1	.987	36.6	1.44	33	48	71.5	65	94.6	86
HAZ, C	73.7	2.9	2.81	0.1105	25.0	0.984	40.4	1.59	32	47	70.4	64	105.6	96
			2.81	.1105	25.1	.990	36.3	1.43	36	52	79.2	72	106.7	97
HAZ, OA	76.2	3.0	2.88	0.1133	24.9	0.982	27.2	1.07	24	35	51.7	47	55.0	50
			2.85	.1123	25.4	1.000	27.2	1.07	24	35	52.8	48	55.0	50
P[c]	25.4	1.0	1.59	0.0625	3.86	0.152	(b)	(b)	101	147	93.5	85	(b)	(b)
			1.59	.0625	5.11	.201	(b)	(b)	90	131	94.6	86	(b)	(b)
	76.2	3.0	1.58	0.0623	25.8	1.015	35.8	1.41	45	65	101.2	92	132.0	120
			1.58	.0622	25.4	1.002	36.6	1.44	45	65	101.2	92	135.3	123
			1.58	.0623	25.6	1.009	36.6	1.44	45	66	102.3	93	135.3	123

[a]P denotes parent metal; W, weld centerline; FL, fusion line; HAZ, heat affected zone; C, chamber weld; OA, open air weld.
[b]Not measured.
[c]Machined from 2.8-millimeter (0.11-in.) sheet.

TABLE V. - SMOOTH PROPERTIES OF PARENT METAL

Temperature		Thickness		Yield strength		Ultimate strength		Elongation in 51 mm (2 in.), percent	Reduction in area, percent
K	°F	mm	in.	kN/cm^2	ksi	kN/cm^2	ksi		
20	-423	1.57	0.0619	156	226	170	247	13	10
		1.56	.0616	156	227	170	247	13	12
		1.58	.0621	159	231	172	249	13	11
Av.	Av.	----	------	157	228	170	247	13	11
77	-320	1.61	0.0634	132	191	138	201	16	27
		1.61	.0633	132	192	139	202	16	24
		1.56	.0616	134	195	139	202	15	26
Av.	Av.	----	------	133	193	139	202	16	25
295	70	1.58	0.0624	83	120	89	129	14	28
		1.60	.0631	81	118	88	128	14	30
Av.	Av.	----	------	82	119	89	129	14	29
20	-423	2.86	0.1126	144	209	152	221	2	(a)
		2.84	.1120	146	212	150	218	2	↓
		2.83	.1114	146	212	159	231	12	↓
		2.82	.1109	145	211	160	233	13	↓
		2.73	.1075	146	212	159	231	9	↓
		2.63	.1037	147	214	156	226	5	↓
Av.	Av.	----	------	146	212	156	227	7	↓
77	-320	2.85	0.1124	123	178	130	189	(a)	(a)
		2.92	.1150	123	178	130	189	19	37
Av.	Av.	----	------	123	178	130	189	19	37
295	70	2.88	0.1133	72	105	79	114	18	43
		2.90	.1143	72	105	78	113	18	44
		2.89	.1138	72	105	78	113	18	43
Av.	Av.	----	------	72	105	78	113	18	43
20	-423	1.60	[b].0628	146	212	160	233	11	(a)

[a]Not measured.

[b]Machined from 2.8 millimeter (0.11 in.) sheet.

TABLE VI. - SMOOTH PROPERTIES OF WELD METAL

Temperature		Type of weld (a)	Thickness		Yield strength		Ultimate strength		Average weld efficiency, percent
K	^{o}F		mm	in.	kN/cm^2	ksi	kN/cm^2	ksi	
20	-423	C	1.63	0.0641	147	213	160	233	94
			1.59	.0625	143	208	159	231	
			1.58	.0621	142	206	160	232	
		Av.	----	------	144	209	160	232	
		OA	1.50	0.0591	145	211	163	237	96
			1.54	.0605	149	216	163	236	
			1.53	.0602	147	214	154	224[b]	
		Av.	----	------	147	214	163	237	
77	-320	C	1.58	0.0624	127	184	136	197	97
			1.57	.0620	123	178	134	195	
			1.58	.0622	123	179	135	196	
		Av.	----	------	124	180	135	196	
		OA	1.55	0.0610	124	180	136	197	98
			1.55	.0611	125	181	136	197	
			1.55	.0611	125	181	136	197	
		Av.	----	------	125	181	136	197	
295	70	C	1.58	0.0622	78	113	88	128	98
			1.55	.0610	78	113	87	126	
			1.59	.0626	74	107	86	125	
			1.58	.0624	73	106	86	125	
		Av.	----	------	76	110	87	126	
		OA	1.52	0.0600	81	117	90	131	100
			1.55	.0612	77	112	88	127	
		Av.	----	------	79	114	89	129	
20	-423	C	2.85	0.1121	138	200	151	219	97
			2.72	.1072	136	197	150	217	
			2.86	.1126	138	201	152	220	
			2.85	.1124	138	200	151	219	
		Av.	----	------	138	200	151	219	
		OA	2.78	0.1095	146	212	156	227	98
			2.92	.1149	147	213	153	222	
			2.81	.1105	148	215	152	221	
		Av.	----	------	147	213	154	223	
77	-320	C	2.87	0.1131	121	175	131	190	100
			2.86	.1125	123	178	131	190	
			2.86	.1125	121	175	130	189	
		Av.	----	------	121	176	130	189	
		OA	2.84	0.1117	123	179	130	188	100
			2.82	.1110	124	180	131	190	
		Av.	----	------	124	180	130	189	
295	70	C	2.92	0.1150	80	116	81	117	104
			2.79	.1100	78	113	81	118	
			2.86	.1125	77	112	81	117	
		Av.	----	------	78	114	81	118	
		CA	2.88	0.1132	76	111	82	119	104
			2.90	.1141	76	110	81	118	
			2.90	.1141	77	112	82	119	
		Av.	----	------	76	111	81	118	

[a]C denotes chamber weld. OA denotes open-air weld.

[b]Not included in average. Porosity detected in fracture surface.